# Appendix: Metabolic oscillations on the circadian time scale in *Drosophila* cells lacking clock genes

Guillaume Rey[1*#], Nikolay B. Milev[1#], Utham K. Valekunja[1], Ratnasekhar Ch[1,2], Sandipan Ray[1,2], Mariana Silva Dos Santos[1], Andras D. Nagy[1], Robin Antrobus[3], James I. MacRae[1], and Akhilesh B. Reddy[1*]

[1] The Francis Crick Institute, 1 Midland Road, London NW1 1AT, UK.
[2] UCL Institute of Neurology, Queen Square, London WC1N 3BG, UK.
[3] Cambridge Institute for Medical Research (CIMR), Wellcome Trust/MRC Building, Addenbrooke's Hospital, Cambridge CB2 0XY, UK.

# Table of contents

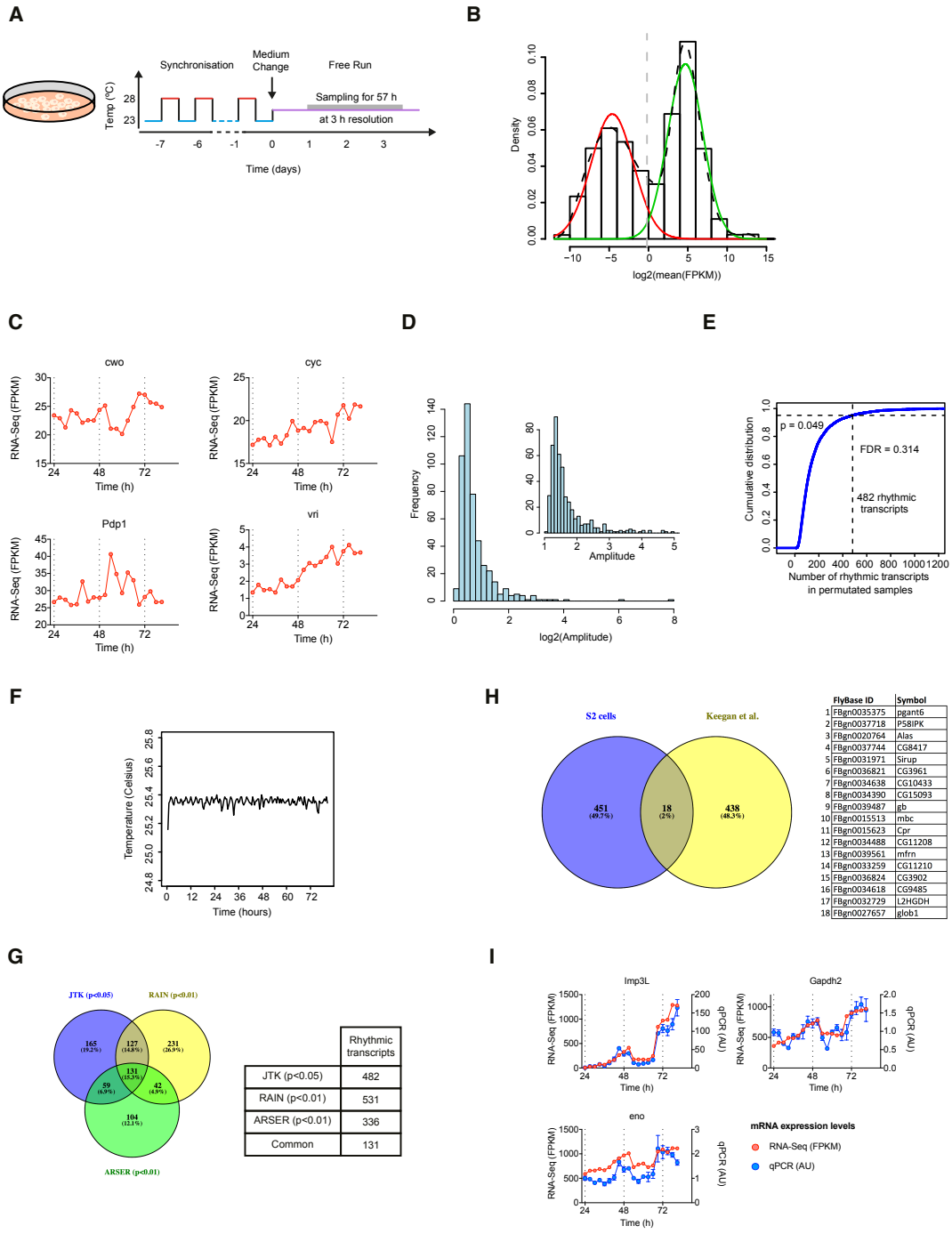


**Appendix Figure S1. RNA-Seq data analysis.**

**A,** Schematic showing the entrainment protocol used to synchronize *Drosophila* S2 cells. **B,** Histogram showing the distribution of mean expression levels measured by RNA-Seq. The distribution was modelled with a mixture model to define the sets of low (red) and highly (green) expressed transcripts. The dashed vertical line represents the cut-off chosen to define the set of expressed transcripts. FPKM, Fragments Per Kilobase of transcript per Million mapped reads. **C,** mRNA expression of four canonical circadian expressed in S2 cells. **D,** Distribution of amplitudes of

the 482 rhythmic transcripts. Amplitudes were calculated by taking the ratio between the maximum and the minimum of each transcript profile. Insert: zoomed version of the plot with a natural scale on the x-axis. **E,** Estimation of FDR using permutation tests. The cumulative distribution of the number of rhythmic transcripts in the 10,000 permutations is shown together with the empirical p-value and estimated FDR. **F,** Temperature recordings inside the incubator chamber show that the temperature is stable and not oscillating during the free-run phase. **G,** Comparison of the JTK-Cycle algorithm with two other methods to detect rhythmic transcripts. A table giving the number of rhythmic transcripts is given (left), together with a Venn diagram showing the overlap between methods (right). **H,** Overlap between the 482 rhythmic transcripts found in the study and the set of 456 rhythmic transcripts compiled from 5 microarray studies (Keegan *et al*, 2007). **I,** Validation of selected transcripts by quantitative PCR (qPCR) (n = 3, mean ± SEM).

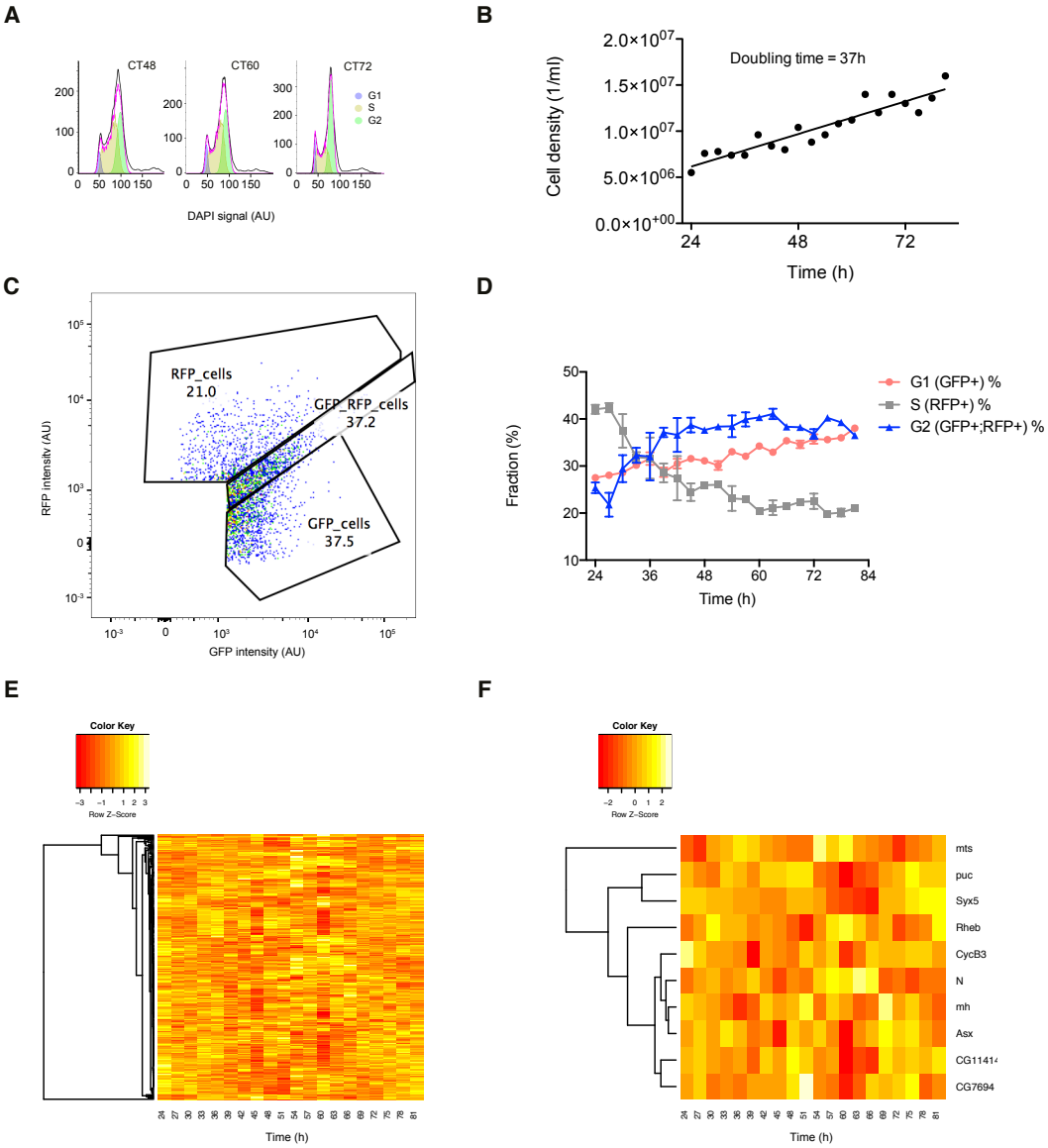


**Appendix Figure S2. Cell cycle analyses in S2 cells.**

**A,** Representative histograms of the DAPI signal at selected time points, with the curve fitting of cell cycle phases. **B,** Cell density of S2 cells during the time course experiment is shown, together with the estimated double time. **C,** Representative image from the flow cytometry analysis of Fly-FUCCI S2 cells showing the windows used to define GFP and RFP positive cells. **D,** Cell cycle analysis of Fly-FUCCI S2 cells using flow cytometry showing the fraction of cells in G1, S and G2 phases over a time course experiment (n = 3 per time-point, mean ± SEM). **E,** Heatmap representation of transcripts with mitotic cell cycle GO annotation from the 25ºC transcriptomics experiment. **F,** Heatmap representation of rhythmic transcripts with mitotic cell cycle GO annotation from the 25ºC transcriptomics experiment.

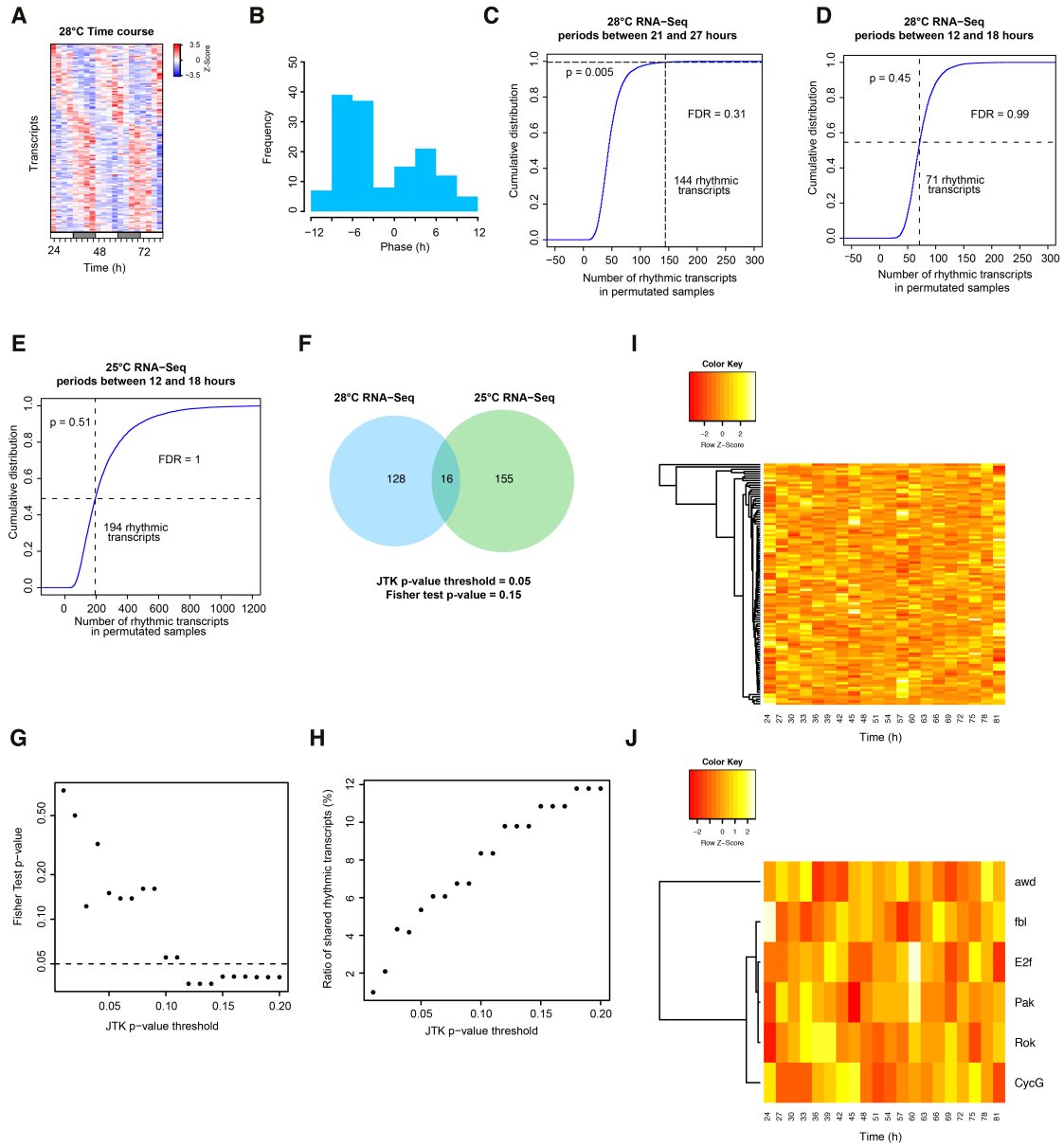


**Appendix Figure S3. RNA-Seq time course at 28°C and temperature compensation.**

**A,** Heatmap showing the expression profiles of the 144 rhythmic transcripts (JTK-Cycle, $p < 0.05$, FDR=0.31) **B,** Distribution of phase of the circadian transcripts shown in **A**. **C, D** Estimation of FDR using permutation tests for JTK analyses for periods of 21-27h (**C**) and 12-18h (**D**). The cumulative distribution of the number of rhythmic transcripts in the 10,000 permutations is shown together with the empirical p-value and estimated FDR. **E,** Estimation of FDR for JTK analyses for periods 12-18h in the 25°C experiment. **F,** Overlap between rhythmic transcripts detected at 25°C and 28°C shown with a Venn diagram. **G,** Statistical significance of the overlap between rhythmic transcripts detected at 25°C and 28°C as a function of the threshold of the JTK algorithm. **H,** Ratio of shared rhythmic transcripts detected at 25°C and 28°C, (# of shared rhythmic transcripts)/(# of rhythmic transcripts detected in either experiment), as a function of the threshold of the JTK algorithm. **I,** Heatmap representation of transcripts with mitotic cell cycle GO annotation from the 28ºC transcriptomics

experiment. **J,** Heatmap representation of rhythmic transcripts with mitotic cell cycle GO annotation from the 28ºC transcriptomics experiment.

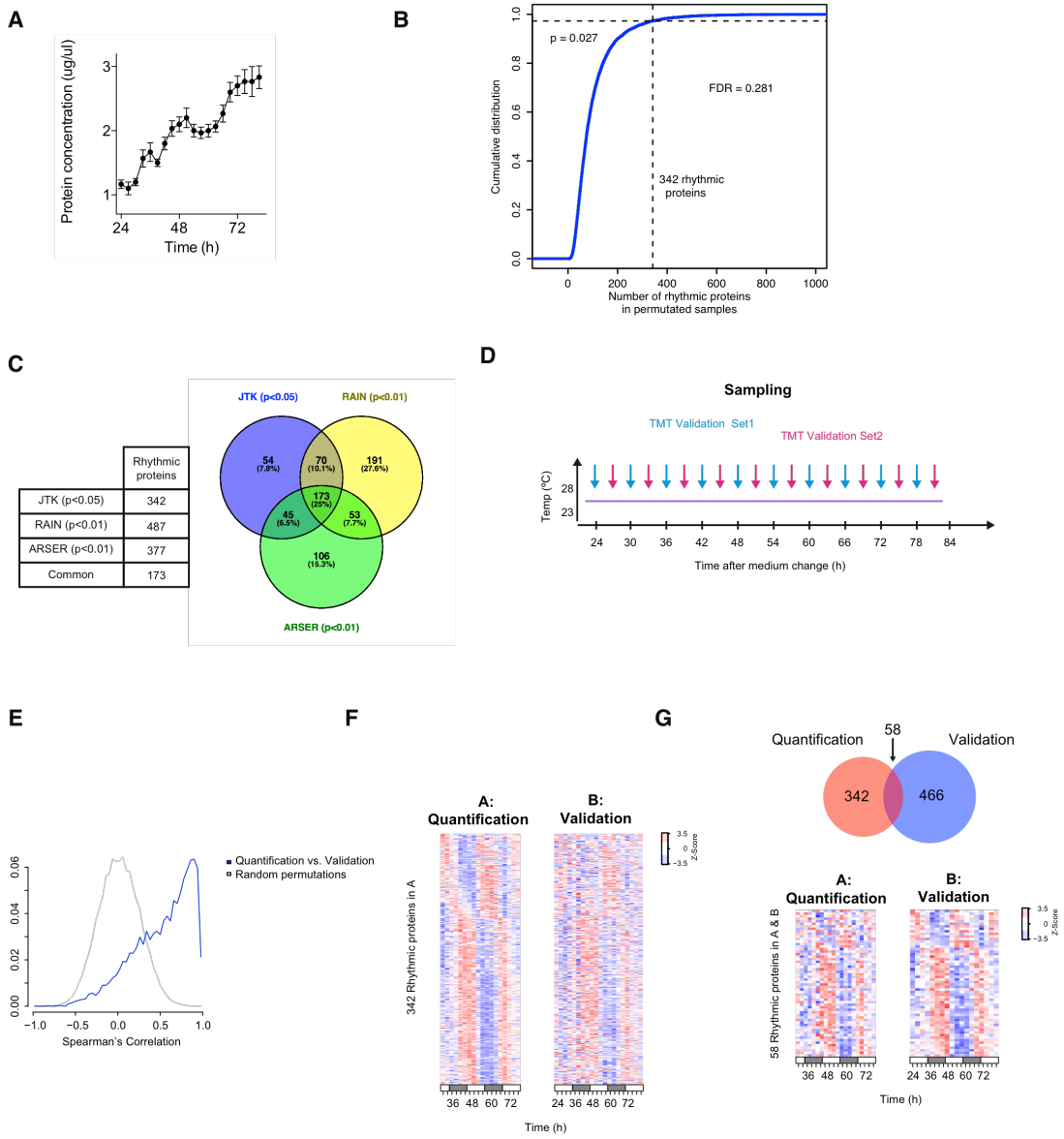


**Appendix Figure S4. Proteomics data analysis.**

**A,** Protein concentration in cell extracts as measured by the BCA method (mean ± SEM, n = 2-3). **B,** Estimation of FDR using permutation tests. The cumulative distribution of the number of rhythmic proteins in the 10,000 permutations is shown together with the empirical p-value and estimated FDR. **C,** Validation of the JTK-Cycle algorithm with two other methods to detect rhythmic transcripts. A table giving the number of rhythmic transcripts is given (left), together with a Venn diagram showing the overlap between methods (right). **D,** Cartoon representing the labelling scheme for the validation protocol. Samples were labelled using interspersed time points (Set 1: CT24, CT30, CT36, …; Set 2: CT27, CT33, CT39, …) and the two 10plex TMTs were then combined to produce 20 time point quantification profiles. **E,** Distributions of Spearman's correlation coefficient between the quantification and validation sets of quantitative proteomics data. Random permutations of the data are shown as control (n = 100). **F,** Heatmap representation of the proteins detected as rhythmic in the

quantification set (342 proteins) for the quantification set (left) and validation set (right). **G,** Heatmap representation of the proteins detected as rhythmic in both the quantification and validation sets (58 proteins) for the quantification set (left) and validation set (right).

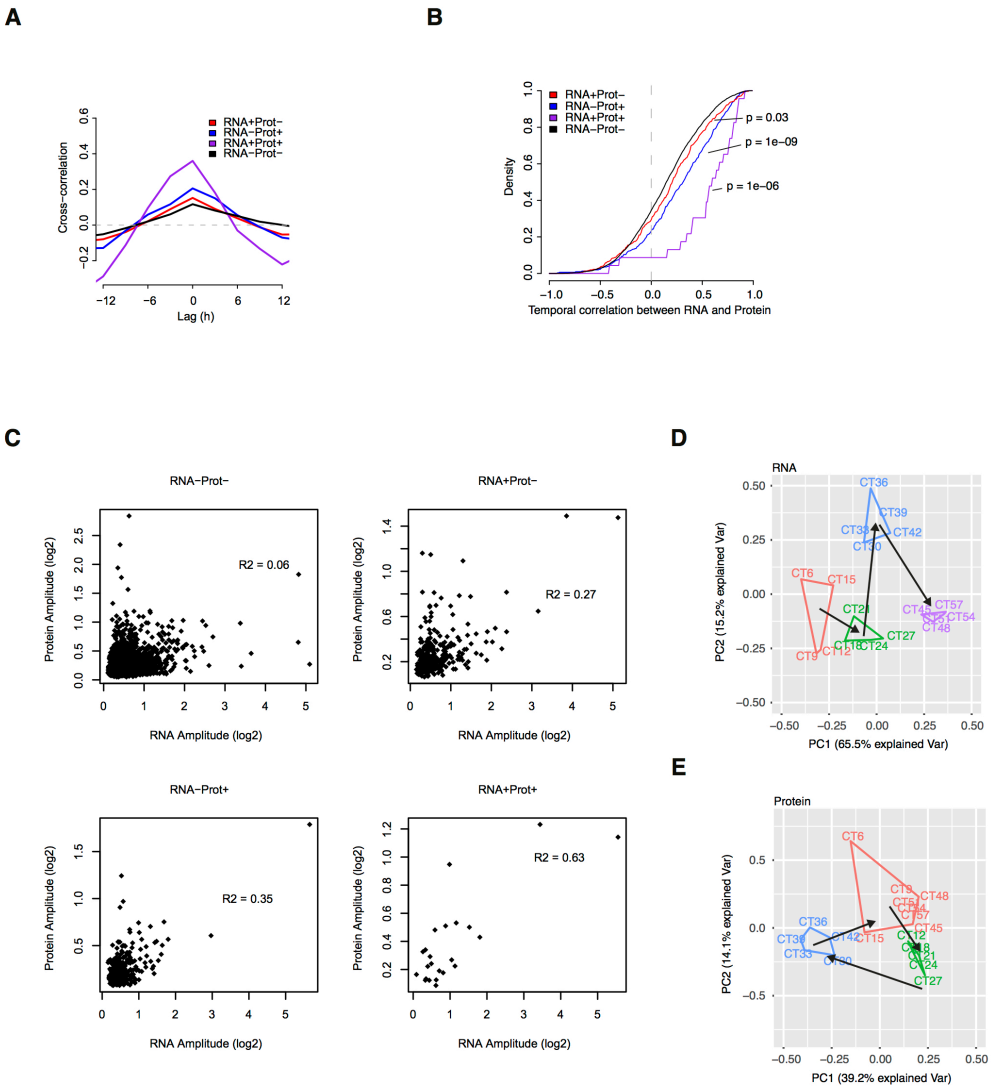


**Appendix Figure S5. Integration of transcriptomics and proteomics data.**

**A,** Temporal cross-correlation for RNA-proteins pairs as described in Figure 3. **B,** Cumulative distributions of Pearson correlation coefficients for the indicated groups of RNA-protein pairs for detrended profiles. RNA-Prot-, neither circadian; RNA+Prot+, both circadian; RNA-Prot+, RNA not circadian and protein circadian; RNA+Prot-, RNA circadian and protein not circadian (Wilcoxon sum rank test). **C,** Scatterplot of amplitude at the transcript and protein levels for the 4 sets of RNA-protein pairs. The coefficient of determination of the linear regression is shown for each comparison. **D, E,** PCA plot of RNA and protein data for all RNA-proteins pairs. Clustering of time points is performed with Partitioning Around Medoids (PAM) method.

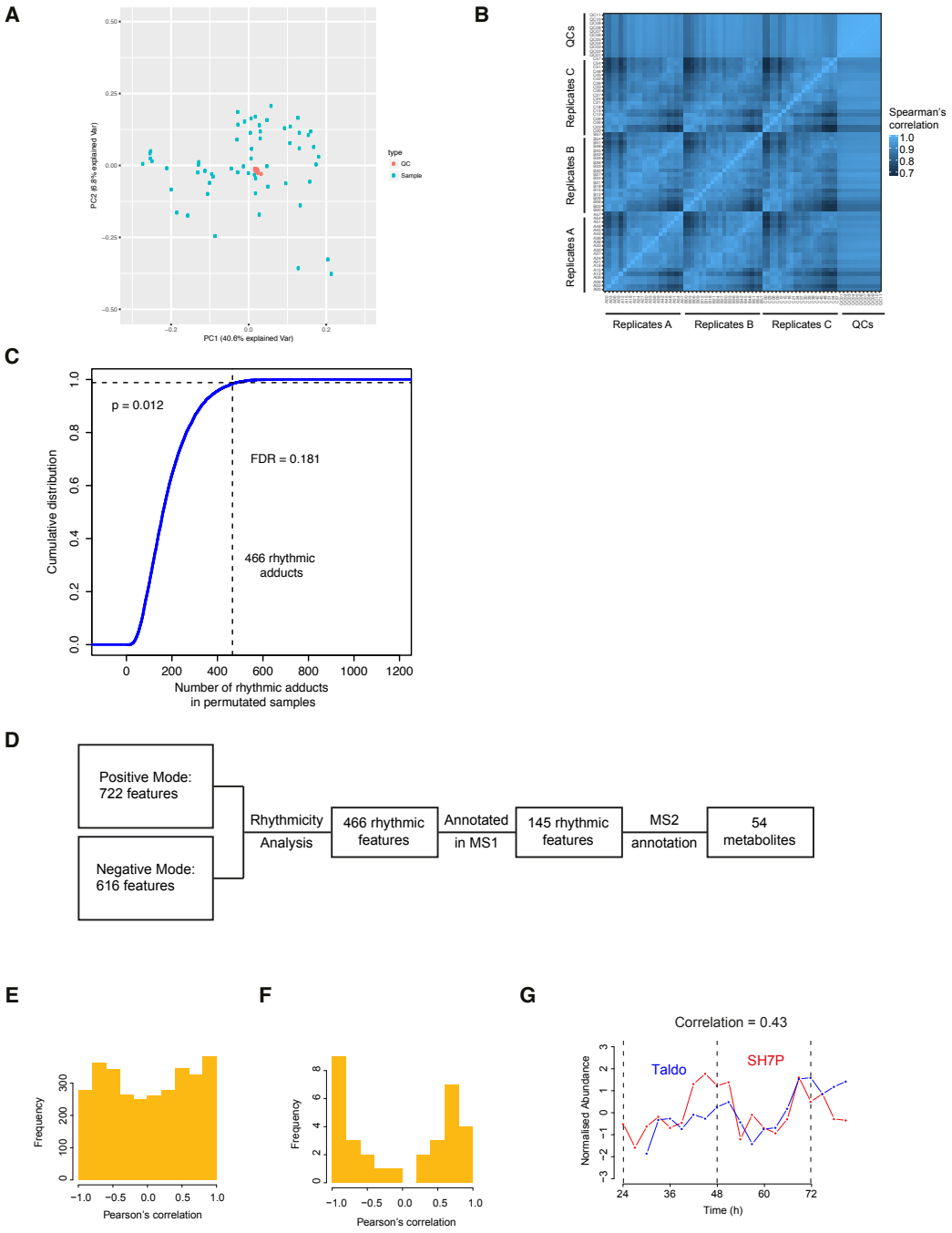


**Appendix Figure S6. Metabolomics data analysis**.

**A,** PCA plot of the 59 samples and 11 quality control (QC) samples analysed in this study. **B,** Heatmap showing the Spearman's correlation between all samples. **C,** Estimation of FDR using permutation tests. The cumulative distribution of the number of rhythmic features in the 10,000 permutations is shown together with the empirical p-value and estimated FDR. **D,** Workflow of untargeted metabolomics data analysis. **E,** Distribution of Pearson's correlation coefficients for all possible protein-metabolite pairs. **F,** Distribution of Pearson's correlation coefficients for the best protein-metabolite pairs. For each metabolite, the correlation coefficients for all possible interacting

proteins were computed and the protein with the highest absolute correlation coefficient was retained. **G,** Examples of correlated protein-metabolites are shown with Pearson correlation coefficient (top). SH7P, sedoheptulose 7-phosphate; Taldo, Transaldolase.

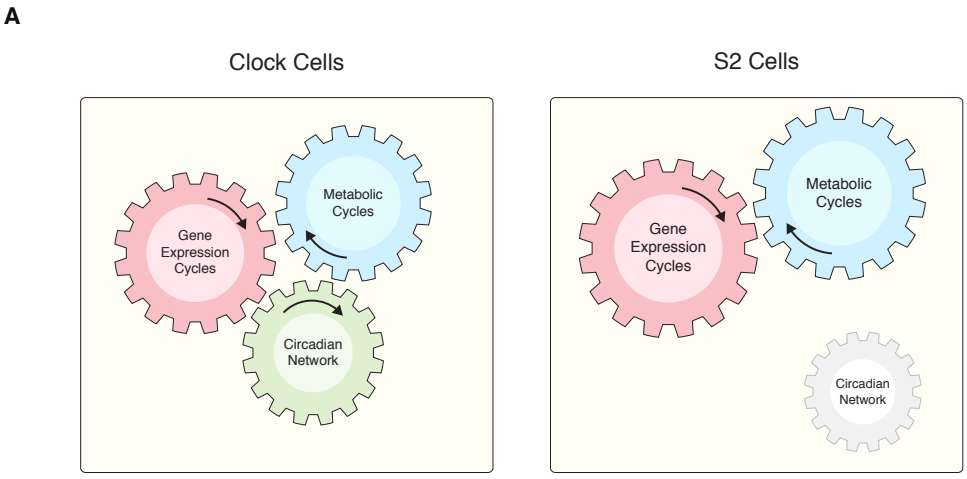


**Appendix Figure S7. Coupled gene expression and metabolic cycles in *Drosophila* S2 cells. A,** Schematic showing the difference between a clock cell where the circadian network is active and *Drosophila* S2 cells, which exhibit gene expression and metabolic cycles in its absence.

## Appendix Table S1.

Table of the 70 MS2-annotated features with m/z, retention time and fragments used for annotation.

| m/z | Retention time (min) | Charge | Polarity | MS2 Annotation | CAS | KEGG | Fragments |
|---|---|---|---|---|---|---|---|
| 132.07 | 12.17 | 1 | Positive | 3-Hydroxy-L-proline | 4298-08-2 | C19706 | 90.06, 132.08 |
| 136.05 | 9.78 | 1 | Positive | Adenine | 73-24-5 | C00147 | 119.04, 92.02, 136.06 |
| 508.00 | 12.85 | 1 | Positive | Adenosine triphosphate | 56-65-5 | C00002 | 136.06, 410.03, 428.04 |
| 118.09 | 10.80 | 1 | Positive | Betaine | 107-43-7 | C00719 | 118.09 |
| 332.14 | 8.15 | 1 | Positive | Ciprofloxacin | 85721-33-1 | C05349 | 231.06, 332.14 |
| 489.11 | 12.79 | 1 | Positive | Citicoline | 987-78-0 | C00307 | 264.04, 184.07 |
| 223.07 | 13.56 | 1 | Positive | Cystathionine | 535-34-2 | C00542 | 134.08, 223.08 |
| 244.09 | 11.22 | 1 | Positive | Cytidine | 65-46-3 | C00475 | 95.02, 112.05 |
| 324.06 | 13.27 | 1 | Positive | cytidine 5-monophosphate | 63-37-6 | C00055 | 112.05, 324.06 |
| 112.05 | 13.27 | 1 | Positive | Cytosine | 71-30-7 | C00380 | 95.02, 112.05 |
| 112.05 | 11.22 | 1 | Positive | Cytosine | 71-30-7 | C00380 | 95.02, 112.05 |
| 148.06 | 12.68 | 1 | Positive | Glutamic acid | 56-86-0 | C00025 | 84.04, 102.06, 130.05 |
| 156.08 | 16.29 | 1 | Positive | Histidine | 71-00-1 | C00135 | 110.07, 113.11,156.08 |
| 127.07 | 11.18 | 1 | Positive | Imizadoleacetic acid | 645-65-8 | | 81.04, 85.05 |
| 88.11 | 10.29 | 1 | Positive | Isoamylamine | 107-85-7 | C02640 | 88.08, 70.07 |
| 170.09 | 7.42 | 1 | Positive | Methyl-L-histidinate | 1499-46-3 | | 110.07, 170.09 |
| 174.11 | 7.10 | 1 | Positive | N-Acetyl-L-leucine | 1188-21-2 | C02710 | 174.06 |
| 664.12 | 12.27 | 1 | Positive | NAD | 53-84-9 | C00003 | 428.04, 136.06, 524.06 |
| 124.04 | 8.08 | 1 | Positive | Niacin | 59-67-6 | C00253 | 124.04, 80.05, 96.04 |
| 166.09 | 10.11 | 1 | Positive | Phenylalanine | 63-91-2 | C00079 | 120.08, 166.09 |
| 166.07 | 9.82 | 1 | Positive | Phenylalanine | 63-91-2 | C00079 | 120.08 |
| 130.09 | 11.47 | 1 | Positive | Pipecolic Acid | 3105-95-1 | C00408 | 84.08, 130.09 |
| 218.14 | 9.86 | 1 | Positive | propionylcarnitine | 17298-37-2 | C03017 | 85.03, 218.14, 159.07 |
| 377.15 | 8.81 | 1 | Positive | Riboflavin | 83-88-5 | C00255 | 243.09 |
| 399.14 | 12.95 | 1 | Positive | S-Adenosyl-L-methionine | 29908-03-0 | C00019 | 250.09, 298.10, 136.06 |
| 106.05 | 13.17 | 1 | Positive | Serine | 56-45-1 | C00065 | 60.04 |
| 203.15 | 14.66 | 1 | Positive | Symmetric Dimethylarginine | 30344-00-4 | | 203.15, 116.07, 70.07, 89.09 |
| 150.11 | 8.86 | 1 | Positive | Triethanolamine | 102-71-6 | C06771 | 70.07, 88.08, 132.10 |
| 183.09 | 12.33 | 1 | Positive | Triethyl phosphate | 78-40-0 | | 98.98, 127.02 |
| 182.08 | 11.89 | 1 | Positive | Tyrosine | 60-18-4 | C00082 | 136.08, 123.04, 119.05, 91.05 |
| 296.08 | 7.13 | 1 | Negative | 5 -S- methyl -5- thioadenosine | 2457-80-9 | C00170 | 134.05 |
| 130.05 | 11.24 | 1 | Negative | 5-aminolevulinic acid | 106-60-5 | C00430 | 130.09 |
| 173.01 | 13.68 | 1 | Negative | Aconitic Acid | 585-84-2 | C00417 | 85.03, 111.01 |
| 505.99 | 12.85 | 1 | Negative | Adenosine triphosphate | 56-65-5 | C00002 | 505.99, 158.92, 408.01, 176.93 |
| 88.04 | 12.70 | 1 | Negative | Alanine | 302-72-7 | C01401 | 88.04 |
| 289.12 | 13.45 | 1 | Negative | Argininosuccinic acid | 2387-71-5 | C03406 | 131.08, 132.03, 173.1 |
| 132.03 | 12.85 | 1 | Negative | Aspartic acid | 56-84-8 | C00049 | 88.04, 71.01, 72.01 |
| 191.02 | 13.75 | 1 | Negative | Citric acid | 77-92-9 | C00158 | 87.01, 111.01, 85.03 |
| 221.06 | 13.56 | 1 | Negative | Cystathionine | 535-34-2 | C00542 | 134.03, 120.01, 221.06 |
| 147.03 | 12.76 | 1 | Negative | D-alpha-Hydroxyglutaric acid | 2889-31-8 | C01087 | 85.03, 101.02, 57.03, 103.04, 129.02 |
| 195.05 | 12.41 | 1 | Negative | D-Gluconic acid | 526-95-4 | C00257 | 75.01, 195.05, 129.02 |
| 171.10 | 7.09 | 1 | Negative | Decanoic acid | 334-48-5 | C01571 | 171.14 |
| 171.10 | 4.44 | 1 | Negative | Decanoic acid | 334-48-5 | C01571 | 171.14 |
| 171.14 | 4.16 | 1 | Negative | Decanoic acid | 334-48-5 | C01571 | 171.14 |
| 121.05 | 11.20 | 1 | Negative | Erythritol | 149-32-6 | C00503 | 71.01, 121.03, 89.02 |
| 259.02 | 13.43 | 1 | Negative | Glucose 6-phosphate | 56-73-5 | C00092 | 96.97, 78.96 |
| 129.02 | 12.76 | 1 | Negative | Glutaconic acid | 1724-02-3 | C02214 | 85.03, 101.02 |
| 146.05 | 12.70 | 1 | Negative | Glutamic acid | 56-86-0 | C00025 | 102.06, 128.03, 146.05 |
| 145.06 | 12.78 | 1 | Negative | Glutamine | 5959-95-5 | C00819 | 101.02, 145.06, 127.05 |
| 152.53 | 12.46 | 2 | Negative | Glutathione | 70-18-8 | C00051 | 74.02, 128.03, 152.87, 86.02 |
| 171.01 | 12.68 | 1 | Negative | Glycerol 3-phosphate | 57-03-4 | C03189 | 78.96, 96.97 |
| 171.08 | 11.65 | 1 | Negative | Glycylproline | 704-15-4 | | 171.14, 96.96 |
| 521.98 | 13.97 | 1 | Negative | Guanosine triphosphate | 86-01-1 | C00044 | 521.98, 424.00 |
| 154.06 | 16.03 | 1 | Negative | Histidine | 150-35-6 | C00135 | 154.06, 137.03, 93.04 |
| 103.00 | 13.03 | 1 | Negative | Malonic acid | 141-82-2 | C00383 | 59.01, 73.03 |
| 181.07 | 13.89 | 1 | Negative | Mannitol | 69-65-8 | C00392 | 181.07, 101.02, 71.01 |
| 181.07 | 12.93 | 1 | Negative | Mannitol | 69-65-8 | C00392 | 181.07, 101.02, 71.01 |
| 181.07 | 14.25 | 1 | Negative | Mannitol | 69-65-8 | C00392 | 181.07, 101.02, 71.01 |
| 172.10 | 4.67 | 1 | Negative | N-Acetyl-L-leucine | 1188-21-2 | C02710 | 172.14, 130.09 |
| 190.05 | 4.93 | 1 | Negative | N-Acetyl-L-methionine | 65-82-7 | C02712 | 84.04 |
| 190.05 | 7.13 | 1 | Negative | N-Acetyl-L-methionine | 65-82-8 | C02713 | 84.04 |
| 122.02 | 8.09 | 1 | Negative | Nicotinic acid | 59-67-6 | C00253 | 94.03, 122.02, 78.03 |
| 164.07 | 10.12 | 1 | Negative | Phenylalanine | 63-91-2 | C00079 | 147.04, 164.07, 72.01 |
| 166.97 | 13.49 | 1 | Negative | Phosphoenolpyruvic acid | 138-38-9 | C00074 | 78.96 |
| 128.07 | 11.50 | 1 | Negative | Pipecolic acid | 535-75-1 | C00408 | 128.03 |
| 117.02 | 12.76 | 1 | Negative | Succinic acid | 110-15-6 | C00042 | 73.03, 117.02, 99.01 |
| 203.08 | 11.08 | 1 | Negative | Tryptophan | 54-12-6 | C00806 | 203.08, 116.05, 159.09 |
| 180.07 | 11.87 | 1 | Negative | Tyrosine | 60-18-4 | C00082 | 180.07, 163.04, 119.05 |
| 167.02 | 11.87 | 1 | Negative | Uric Acid | 13154-20-6 | C00366 | 69.01, 124.01, 96.02 |
| 151.03 | 11.20 | 1 | Negative | Xanthine | 69-89-6 | C00385 | 151.03, 108.02, 136.02 |

**Appendix Table S2.**

Table of the 20 metabolites selected for targeted LC-MS analysis.

| m/z | Polarity | RT Start (min) | RT End (min) | Name | Abbreviation |
|---|---|---|---|---|---|
| 261.037 | Positive | 12.8 | 13.8 | Glucose 6-phosphate | G6P |
| 308.0911 | Positive | 11.8 | 12.8 | Glutathione reduced | GSH |
| 348.07036 | Positive | 11.5 | 12.5 | Adenosine monophosphate | AMP |
| 428.0367 | Positive | 11.9 | 12.9 | Adenosine diphosphate | ADP |
| 508.00304 | Positive | 12.4 | 13.4 | Adenosine triphosphate | ATP |
| 613.1593 | Positive | 12.8 | 13.8 | Glutathione oxidized | GSSG |
| 664.11641 | Positive | 11.1 | 12.1 | Nicotinamide adenine dinucleotide | NAD |
| 744.08272 | Positive | 12.4 | 13.4 | Nicotinamide adenine dinucleotide phosphate | NADP |
| 89.02441 | Negative | 9.5 | 10.5 | Lactic acid | Lac |
| 115.0037 | Negative | 12.5 | 13.5 | Fumaric acid | Fum |
| 117.01933 | Negative | 12.2 | 13.2 | Succinic acid | Succ |
| 133.0143 | Negative | 12.5 | 13.5 | Malic acid | Mal |
| 145.0143 | Negative | 12.1 | 13.1 | Alphaketoglutaric acid | a-KG |
| 166.9751 | Negative | 12.9 | 13.9 | Phosphoenolpyruvic acid | PEP |
| 168.9908 | Negative | 12.2 | 13.2 | DHAP | DHAP |
| 191.0197 | Negative | 13.1 | 14.1 | (Iso)citrate | (Iso)cit |
| 229.0119 | Negative | 12.4 | 13.4 | Ribose 5-phosphate/Ribulose 5-phosphate | R5P/Ru5P |
| 259.0224 | Negative | 12.8 | 13.8 | Fructose 6-phosphate | F6P |
| 289.033 | Negative | 12.5 | 13.5 | Sedoheptulose 7-phosphsate | SH7P |
| 338.9888 | Negative | 13 | 14 | Fructose 1,6-biphosphate | FBP |